

Consecutive light microscopy, scanning-transmission electron microscopy and transmission electron microscopy of traumatic human brain oedema and ischaemic brain damage

O.J. Castejon, H.V. Castejon, M. Diaz and A. Castellano

Institute of Biological Researchs, School of Medicine, University of the Zulia, Maracaibo, Venezuela

Summary. Cortical biopsies of 11 patients with traumatic brain oedema were consecutively studied by light microscopy (LM) using thick plastic sections, scanning-transmission electron microscopy ((S)TEM) using semithin plastic sections and transmission electron microscopy (TEM) using ultrathin sections. Samples were glutaraldehyde-osmium fixed and embedded in Araldite or Epon. Thick sections were stained with toluidine-blue for light microscopy. Semithin sections were examined unstained and uncoated for (S)TEM. Ultrathin sections were stained with uranyl and lead. Perivascular haemorrhages and perivascular extravasation of proteinaceous oedema fluid were observed in both moderate and severe oedema. Ischaemic pyramidal and non-pyramidal nerve cells appeared shrunken, electron dense and with enlargement of intracytoplasmic membrane compartment. Notably swollen astrocytes were observed in all samples examined. Glycogen-rich and glycogen-depleted astrocytes were identified in anoxic-ischaemic regions. Dark and hydropic satellite, interfascicular and perivascular oligodendrocytes were also found.

The status spongiosus of severely oedematous brain parenchyma observed by LM and (S)TEM was correlated with the enlarged extracellular space and disrupted neuropil observed by TEM. The (S)TEM is recommended as a suitable technique for studying pathological processes in the central nervous system and as an informative adjunct to LM and TEM.

Key words: Light microscope, Scanning-transmission electron microscopy, Transmission electron microscopy, Nerve cells, Blood-brain barrier

Introduction

Comparative and correlative observations by light microscopy, scanning-transmission electron microscopy and transmission electron microscopy have been widely performed in biology, histology and pathology in a large variety of tissue (Scott et al., 1975; De Nee et al., 1977; Kushida et al., 1977; Sturrock, 1978, 1979, 1984; Tannenbaum et al., 1978; Mikel and Johnson, 1980; Ogura and Laudate, 1980; Boyde and Reid, 1983; Nagato et al., 1983; Pasquinelli et al., 1985; Cajander, 1986; Pavlick et al., 1986; Oka et al., 1987; Wouters, 1987; Ito et al., 1988; Brockmeyer et al., 1989; Scala et al., 1990, 1991; Tolviva et al., 1994; Wergin et al., 1997; Phillips, 1998).

Scanning-transmission electron microscopy ((S)TEM), which implies transmission electron microscopy (TEM) performed with a scanned, focused electron beam, allows us to explore a semithin section in a raster-like form. A fine electron probe is passed across the semithin specimen and the intensity of the transmitted electron signal is measured using one or more electron detectors (Keyse et al., 1998). An image is then built up point by point, just as in a conventional scanning electron microscope. This image could be correlated with the thick section of an optical microscope image and consecutively examined by ultrathin section for TEM. In the present paper we report the potential contribution of a combined light microscope (LM), (S)TEM and TEM study applied to the oedematous human cerebral cortex, using thick,

semithin and ultrathin sections of plastic-embedded cortical biopsies. To the best of our knowledge, such an intermicroscopy approach has not been simultaneously carried out in human oedematous cerebral cortex.

Materials and methods

Samples of cerebral cortex of 11 patients with complicated traumatic head injuries were used in the present study. Cortical biopsy was performed during surgery according to the basic principles of the Helsinki Declaration. According to the intensity of traumatic injury, clinical symptoms and macroscopic observations in the neurosurgical clinic, patients were classified by the neurosurgeon into moderate and severe brain oedema. At light microscopy level the severe oedema was characterized by the status spongiosus of brain parenchyma. At the transmission electron microscopy level, moderate and severe oedema were distinguished by the degree of enlargement of extracellular space (Castejón et al., 1997). Quantitative data by

computerized tomography examination were not performed. Clinical data, diagnosis, biopsy region and degree of brain oedema appear listed in Table 1.

Cortical biopsies, 2-5 mm thick, were immediately fixed in the surgical room in 4% glutaraldehyde-0.1M phosphate or cacodylate buffer, pH 7.4 at 4 °C. They were later, divided into 1 mm fragments and immersed in a similar fresh solution for periods varying from 2 to 72 h, followed by secondary fixation in 1% osmium tetroxide-0.1M phosphate buffer, pH 7.4 for 1 h. They were then rinsed 5 to 10 min in a buffer similar to that used in the fixative solution, dehydrated in increasing concentrations of ethanol and embedded in Araldite or Epon. For light microscopy, thick sections of approximately 0.1 to 1 µm obtained with an LKB pyramitome were stained with toluidine blue and examined with a Zeiss photomicroscope. Uncoated and unstained semithin sections obtained with a Porter-Blum ultramicrotome were observed in a JEOL 100B equipped with an ASID high resolution scanning attachment and

Table 1. Clinical data, diagnosis, biopsy region and degree of brain oedema.

CASE NO.	AGE AND SEX	CLINICAL DATA	DIAGNOSIS	OEDEMA	BRAIN CORTICAL BIOPSY
1. PMD (CCH27)	21 years, male	Fall from a light post, coma, bilateral papilledema	Right epidural haematoma	Severe	Right temporal cortex
2. JP. (CCH29)	14 years, male.	Contusion and fracture of frontal region, transitory loss of consciousness	Contusion and fracture of frontal region	Moderate	Left frontal cortex
3. H.R.F. (CCH17)	18 years, female	Severe frontal contusion in road accident, loss of consciousness; convulsive crisis.	Severe frontal contusion	Severe	Left frontal cortex
4. J.R. C.R. (CCH31)	80 years, male	After suffering fall, chronic alcoholic presented headache, diminution of muscle strength of lower extremities and right arm, temporary loss of consciousness, dysarthria, anisocoria	Left frontoparietal-occipital subdural haematoma	Moderate	Left parietal cortex
5. J.M. (CCH21)	56 years, male	Clouded sensorium, temporospatial disorientation; left mydriasis	Contusion and haematoma of left parietotemporal region	Moderate	Left parietotemporal cortex
6. O.P. (CCH30)	60 years, female	Head injury in traffic accident, fracture of both legs, state of coma, abolition of reflexes; left midriasis; after recovery showed disorders of behaviour (post-traumatic confusional syndrome).	Subdural hygroma	Severe	Right parietal cortex
7. A.V.N.G. (CCH18)	39 years, male	Loss of consciousness after fall from a truck, headache; left hemiparesis, papilloedema	Right parietotemporal haematoma	Severe	Right parietal cortex
8. A.S.C.R. (CCH 22)	26 years, male	Skull trauma in right temporo-parietal cortex, tonicclonic convulsions, disorder of behaviour	Right parietotempora haematoma	Severe	Right temporo-parietal cortex
9. LGH (CCH15)	10 years, female	Fracture of skull in left parietal region	Brain trauma and left parietal extradural haematoma	Severe	Posterior parietal cortex
10. JM (CCH21)	58 years, male	Contusion and haematoma of left parieto-temporal region, clouded sensorium, temporospatial disorientation left mydriasis.	Brain trauma. Left parieto-occipital subdural hygroma	Moderate	Left parieto-temporal cortex
11. LCS (CCH63)	20 years, female	Frontal headache	Brain trauma. Left frontal haematoma	Severe	Left frontal cortex.

aligned in the (S)TEM mode. Ultrathin sections obtained with Porter-Blum and LKB ultramicrotomes, were stained with uranyl acetate and lead citrate and examined in a JEOL 100B transmission electron microscope. Observations were made using intermediate magnifications ranging from x30,000-60,000.

Results

The LM study of moderately oedematous parietal cortex using thick plastic sections, showed pericapillary haemorrhages (Fig. 1) and formation of large pericapillary spaces. Examination of the brain

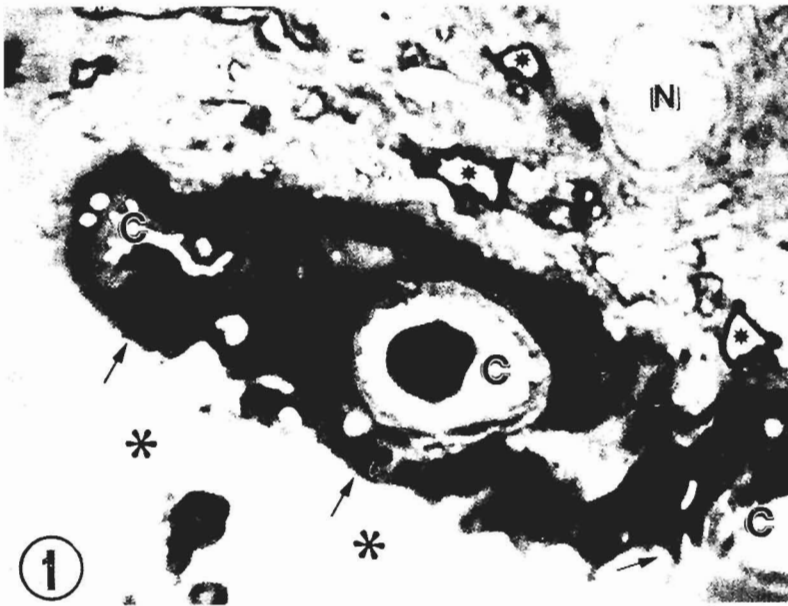


Fig. 1. Case No. 4. Left frontoparietal-occipital subdural haematoma. Photomicrograph of a thick section of moderately oedematous left parietal cortex stained with toluidine blue. A perivascular haemorrhage (arrows) appears completely surrounding three capillaries (C). A pale swollen nerve cell (N) and degenerated myelinated axons (small asterisks) are also observed. Note the neighbouring translucent perivascular space (large asterisks). x 512

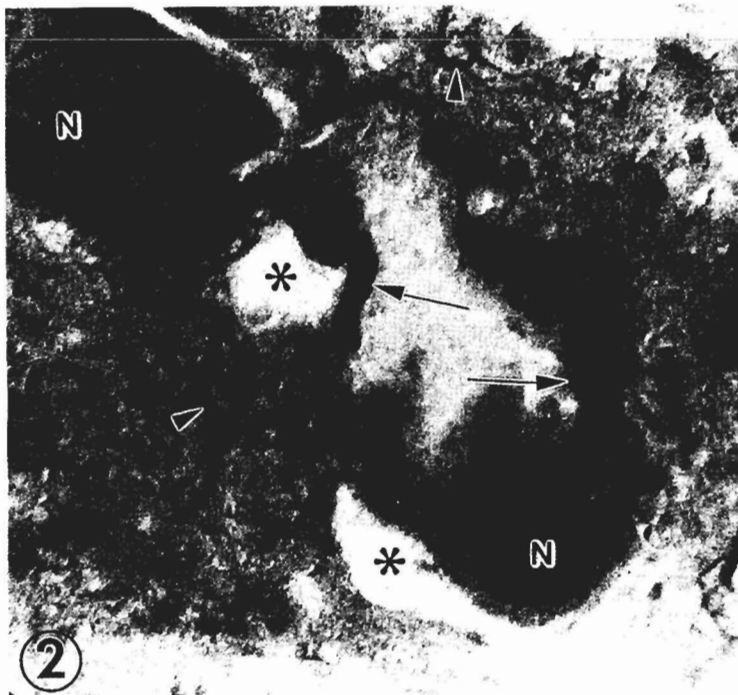


Fig. 2. Case No. 5. Contusion and haematoma of left parieto-temporal region. Moderate oedema. Transmission-scanning electron micrograph of an unstained semithin section of parietal cortex showing a partially collapsed capillary. The nuclear (N) regions of two endothelial cells and their peripheral endothelial cytoplasm (arrows) are distinguished. Large electron translucent perivascular spaces (asterisks) appear surrounding the capillary wall. Some degenerated myelinated axons (arrowheads) are also seen in the perivascular neuropil. x 2,500



Fig. 3. Case No. 3. Severe frontal contusion. Left frontal cortex. Severe oedema. Ultrathin section of a disrupted capillary wall showing perivascular hemorrhages with extravasated erythrocytes (E) and proteinaceous oedema fluid (EF). The capillary wall shows the nuclear (Nu) and peripheral endothelial (PE) regions. The arrows indicate the invagination of endothelial cell luminal plasma membrane to form pinocytotic vesicles (arrowheads) and vacuoles (v). The basement membrane (BM) appears thickened. A segment of pericyte cell cytoplasm (PC) is also observed. x 60,000

parenchyma showed moderate oedema of neuropil characterized by ischaemic, shrunken, dense pyramidal and non-pyramidal nerve cells, dense satellite oligodendrocytes and degenerated, bead-shaped myelinated axons.

Examination by means of (S)TEM of the perivascular region, using semithin, unstained, plastic

sections (Fig. 2), allowed us to clearly visualize the electron translucent perivascular spaces surrounding the capillary wall, indicating the blood brain-barrier breakdown and the extravasation of proteinaceous oedema fluid. Ultrathin sections of the pericapillary haemorrhages showed the extravasated erythrocytes surrounded by a dense haematogenous oedema fluid

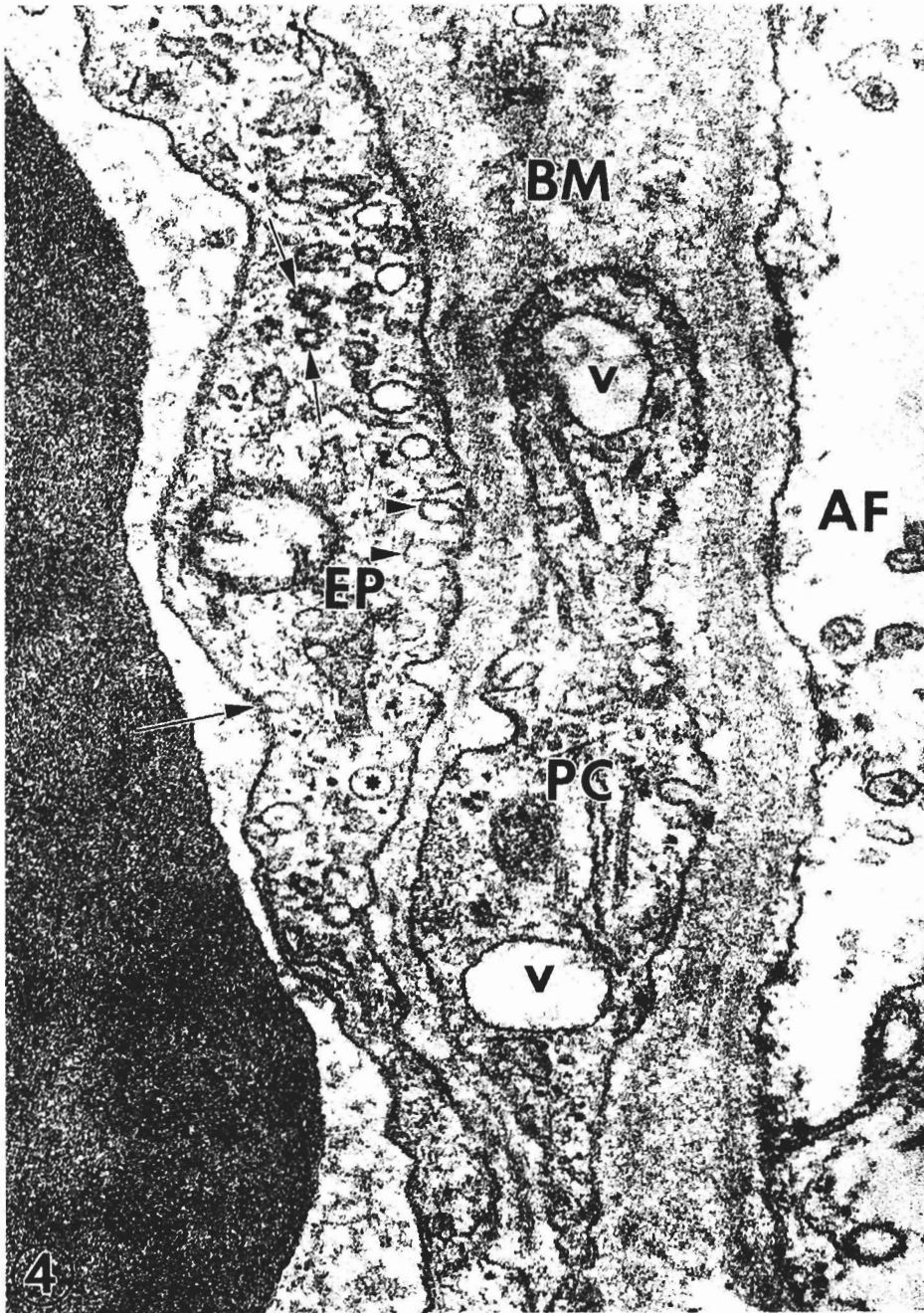


Fig. 4. Case No. 6. Subdural hygroma. Right-parietal cortex. Severe oedema. Ultrathin section of endothelial cell peripheral cytoplasm (EP) showing increased amount of micro and macropinocytotic vesicles. They are observed forming at the luminal plasma membrane (arrow), moving across the endothelial cytoplasm (asterisk) and discharging (arrowheads) at the swollen hydrated basement membrane (BM). Coated vesicles are also seen (short arrows). The perivascular swollen astrocytic end-feet (AF) appear associated to the basement membrane outer surface. The pericyte cytoplasm (PC) enclosed within the basement membrane bifurcations also exhibits vacuolar (v) transport. x 60,000

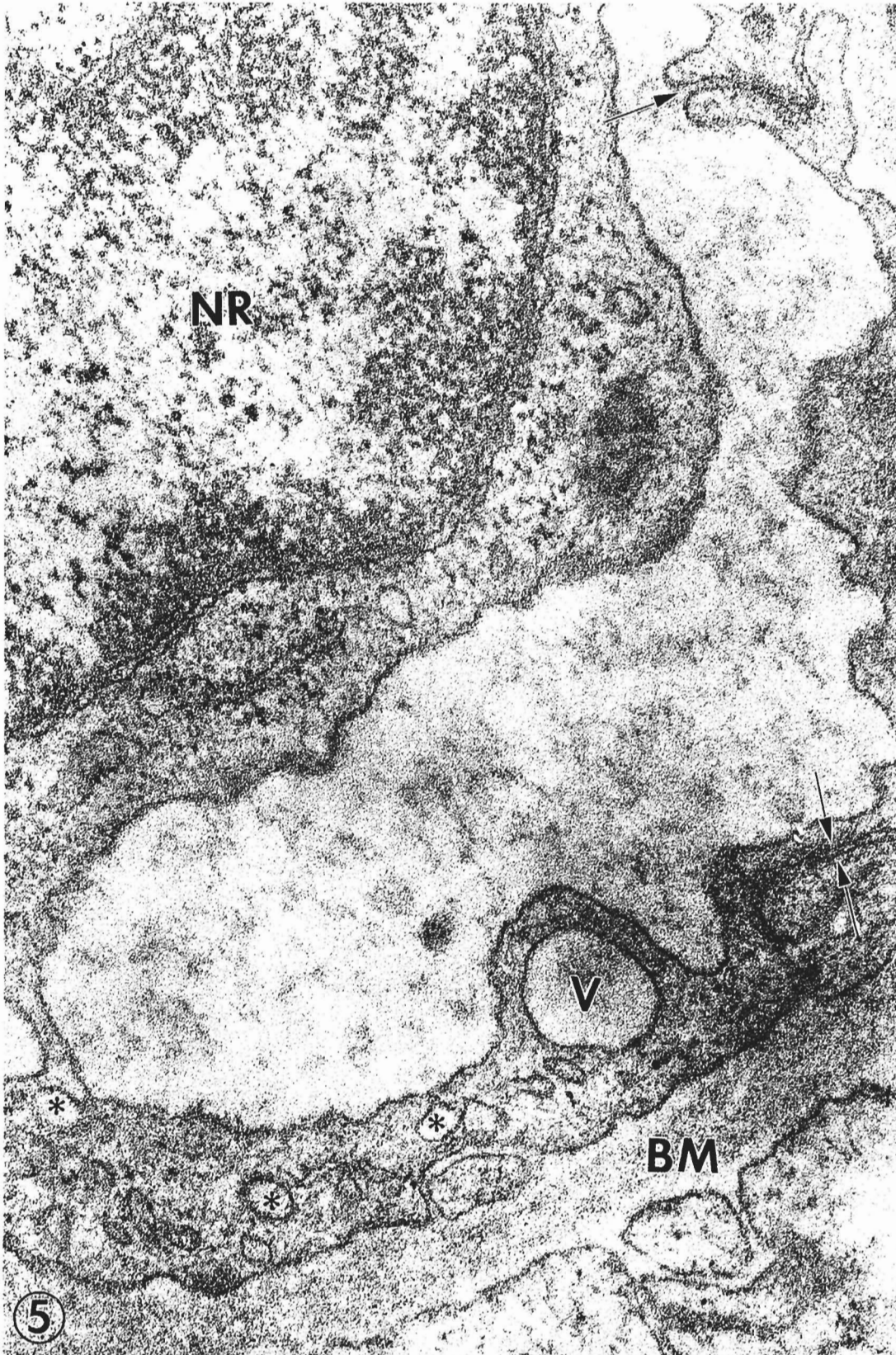


Fig. 5. Case No. 7. Right parietotemporal haematoma. Right parietal cortex. Severe oedema. Ultrathin section of a cross-sectioned partially collapsed capillary showing the prominent nuclear region (NR) and the open endothelial junctions (arrows). A vacuole (V) and pinocytotic vesicles (asterisks) are seen in the peripheral endothelial cytoplasm. The basement membrane (BM) shows rarefaction and thickening. x 60,000

(Fig. 3). The capillary wall showed signs of increased cerebrovascular permeability featuring invaginations of endothelial cell luminal plasma membrane, and an oedematous, thickened basement membrane. Close examination of the endothelial cell peripheral zone (Fig. 4) showed an increased transcytosis process, characterized by increased amount of micropinocytotic vesicles and vacuoles, forming at the luminal front, moving through the endothelial cytoplasm and discharging toward the basement membrane. A similar

transcytosis process was also observed in the pericytal cell enclosed within the capillary basement membrane.

Some partially collapsed capillaries showed a prominent endothelial cell nuclear zone, increased vesicular and vacuolar transport and open endothelial junctions (Fig. 5). Light microscopy of a thick section of the moderately oedematous parietal cortex showed severe ischaemic dense pyramidal and non-pyramidal nerve cells, dense oligodendrocytes and associated degenerated myelinated axons (Fig. 6). Examination of

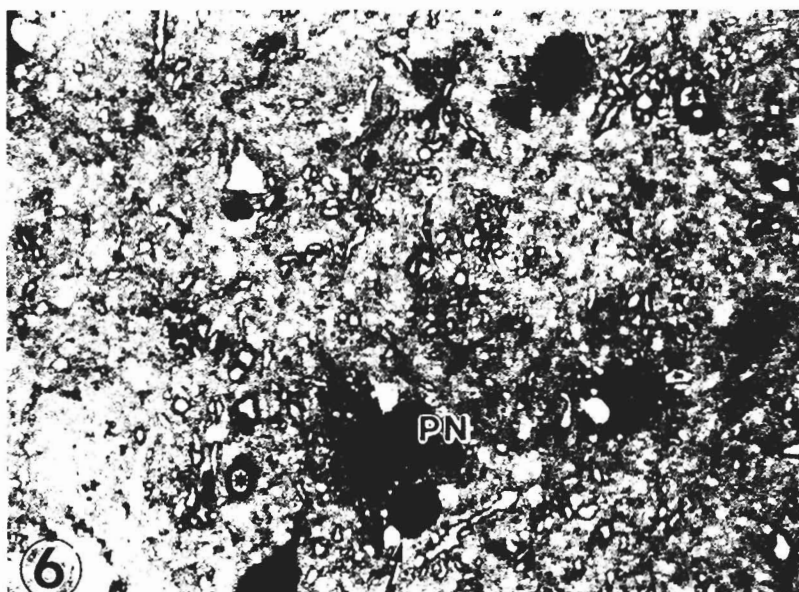


Fig. 6. Case No. 10. Left parieto-occipital subdural hygroma. Left parietal cortex. Photomicrograph of an Epon thick section stained with toluidine blue. Moderately oedematous left parietal cortex showing a shrunken, degenerated pyramidal nerve cell (PN), a dense satellite oligodendrocyte (arrow) and degenerated myelinated axons (asterisks), x 640

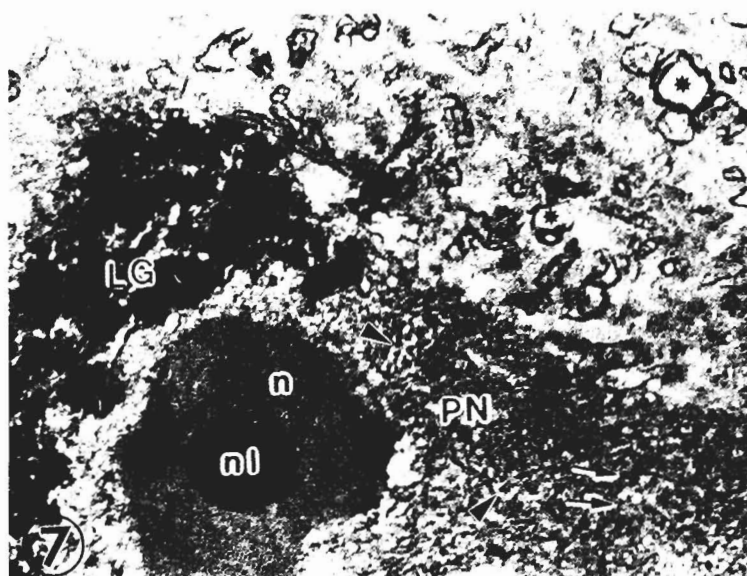


Fig. 7. Case No. 10. Left parieto-occipital subdural hygroma. Left parietal cortex. Moderate oedema. Scanning-transmission electron micrograph of an Epon unstained semithin section. A swollen pyramidal nerve cell (PN) at higher resolution and magnification shows the dense nucleus (n) and denser nucleolus (nl), a huge deposit of lipofuscin granules (LG) and vaguely discerned profiles of distended endoplasmic reticulum (arrowheads). The arrows indicate the emergence of an apical dendrite. Degenerated myelinated axons are observed in the neighbouring oedematous neuropil (asterisks), x 2,500

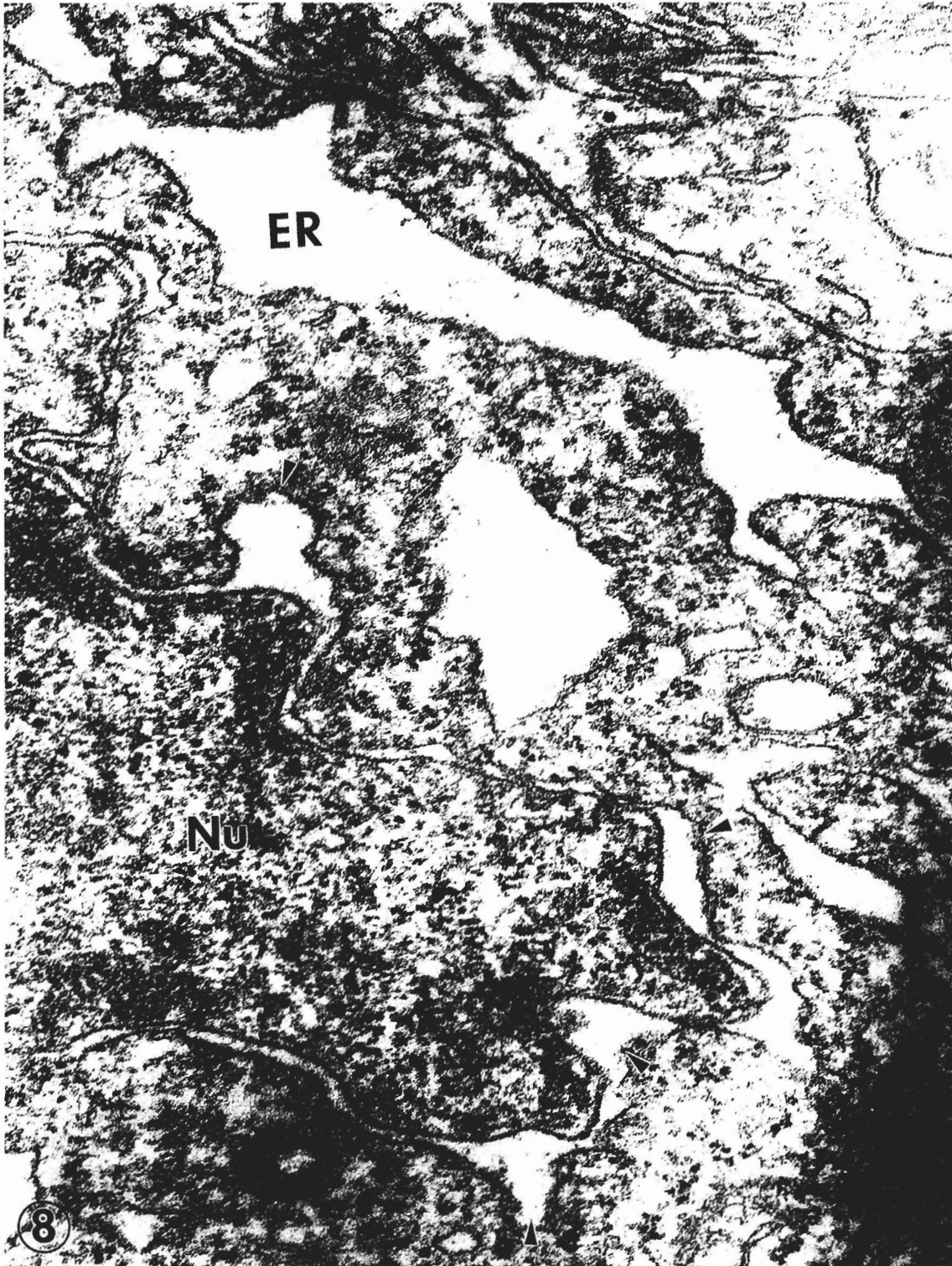


Fig. 8. Case No. 7. Right parieto-temporal haematoma. Ultrathin section of an oedematous pyramidal neuron of right parietal cortex showing notable enlargement of endoplasmic reticulum (ER) and perinuclear cisterns (arrowheads). The nucleus (Nu) shows deep invaginations. x 60,000

this region with (S)TEM showed higher resolution images of ischaemic neurons and the intraneuronal oedema characterized by distended endoplasmic reticulum profiles (Fig. 7); TEM examination at higher magnification of ultrathin sections showed the enlargement of neuronal membrane compartment induced by the intracellular oedema (Fig. 8).

Light microscopy of notably oedematous right temporal cortex using thick sections, showed the classically described status spongiosus of brain parenchyma, that featured severe oedema and notably

swollen astrocyte cells (Fig. 9). Examination of the same region by means of (S)TEM, using unstained semithin sections, showed at higher resolution swollen oedematous astrocyte and vacuolar disruption of severely oedematous brain parenchyma (Fig. 10). Close TEM examination of these severely oedematous regions by means of ultrathin sections showed lacunar enlargement of the extracellular space, containing non-proteinaceous oedema fluid (Fig. 11). The oedema fluid dissociated the nerve cell processes in the neuropil forming lacunar enlargement of extracellular spaces.

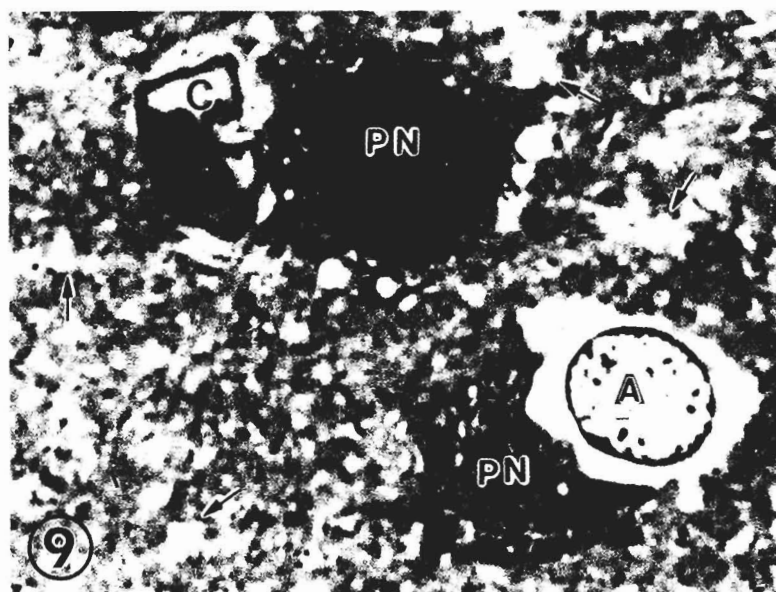


Fig. 9. Case No. 8. Right parieto-temporal haematoma. Photomicrograph of an Epon thick section. Right temporo-parietal cortex stained with toluidine blue. A notably oedematous perineuronal astrocyte (A) appears surrounding a shrunken pyramidal neuron (PN). Note the vacuolar aspect or status spongiosus of brain parenchyma in severe oedema (short arrows). Another ischaemic pyramidal nerve cell (PN) is seen in the vicinity of a capillary (C). x 930

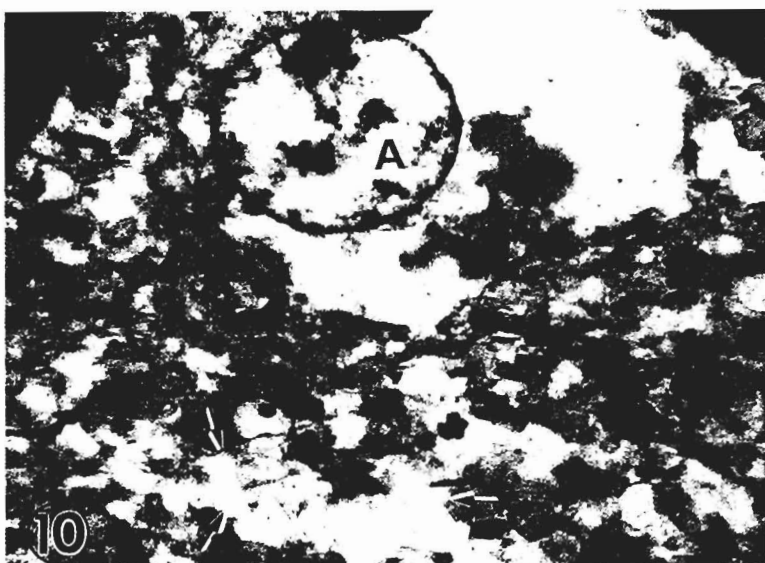


Fig. 10. Case No. 8. Right parieto-temporal haematoma. Scanning-transmission electron micrograph of an Epon unstained semithin section of posterior parietal right temporal cortex with severe oedema. A remarkably swollen astrocyte (A) is observed in the vicinity of a disrupted neuropil, in which large distended extracellular spaces (short arrows) are distinguished. x 2,500

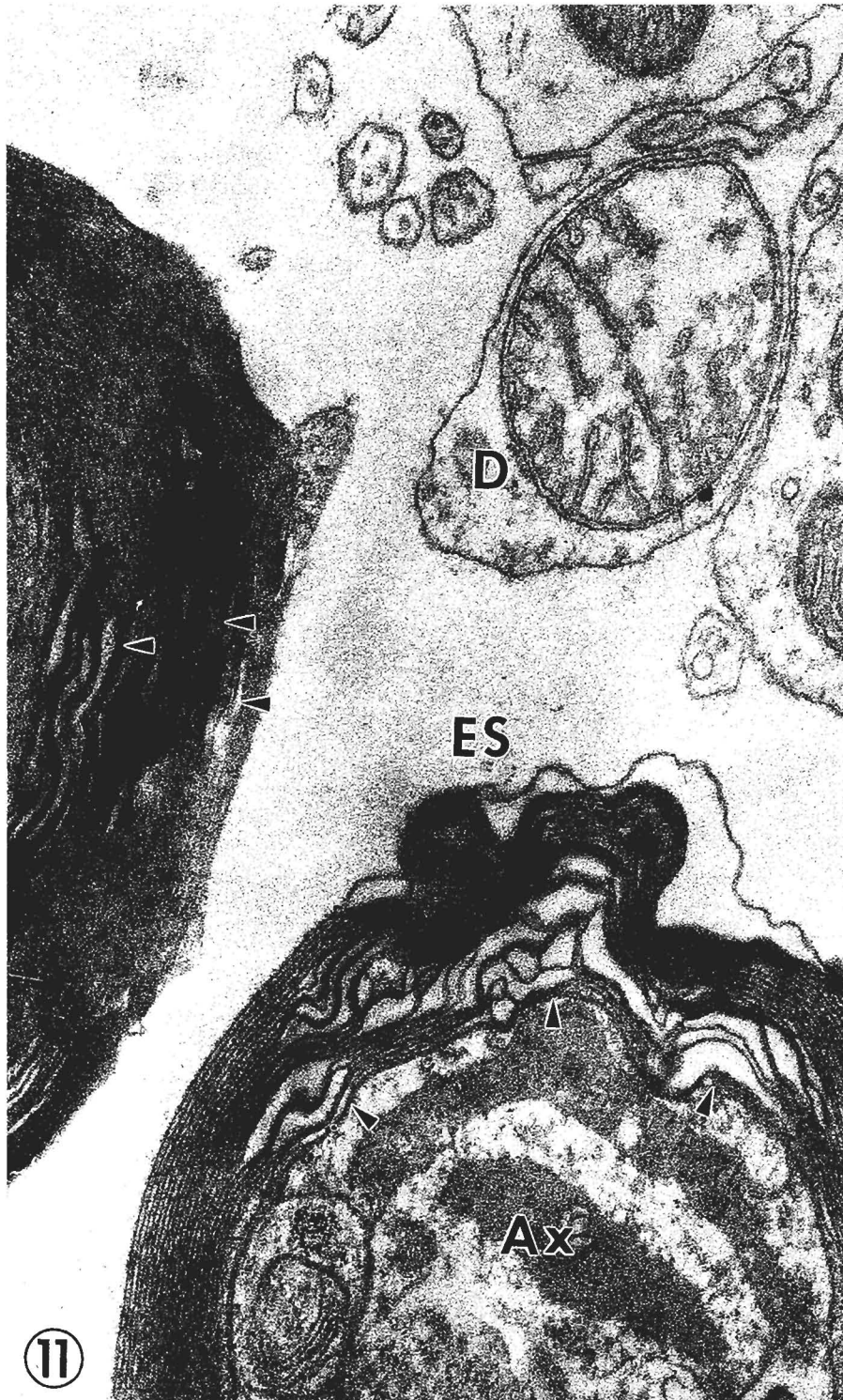


Fig. 11. Case No. 9. Left parietal extradural haematoma. Left parietal cortex. Severe oedema. Ultrathin section of remarkably oedematous neuropil showing lacunar enlargement of extracellular space (ES), containing non-proteinaceous oedema fluid separating degenerated myelinated axons (Ax) and swollen dendritic processes (D). Note the myelin sheath disruption (arrowheads). x 60,000

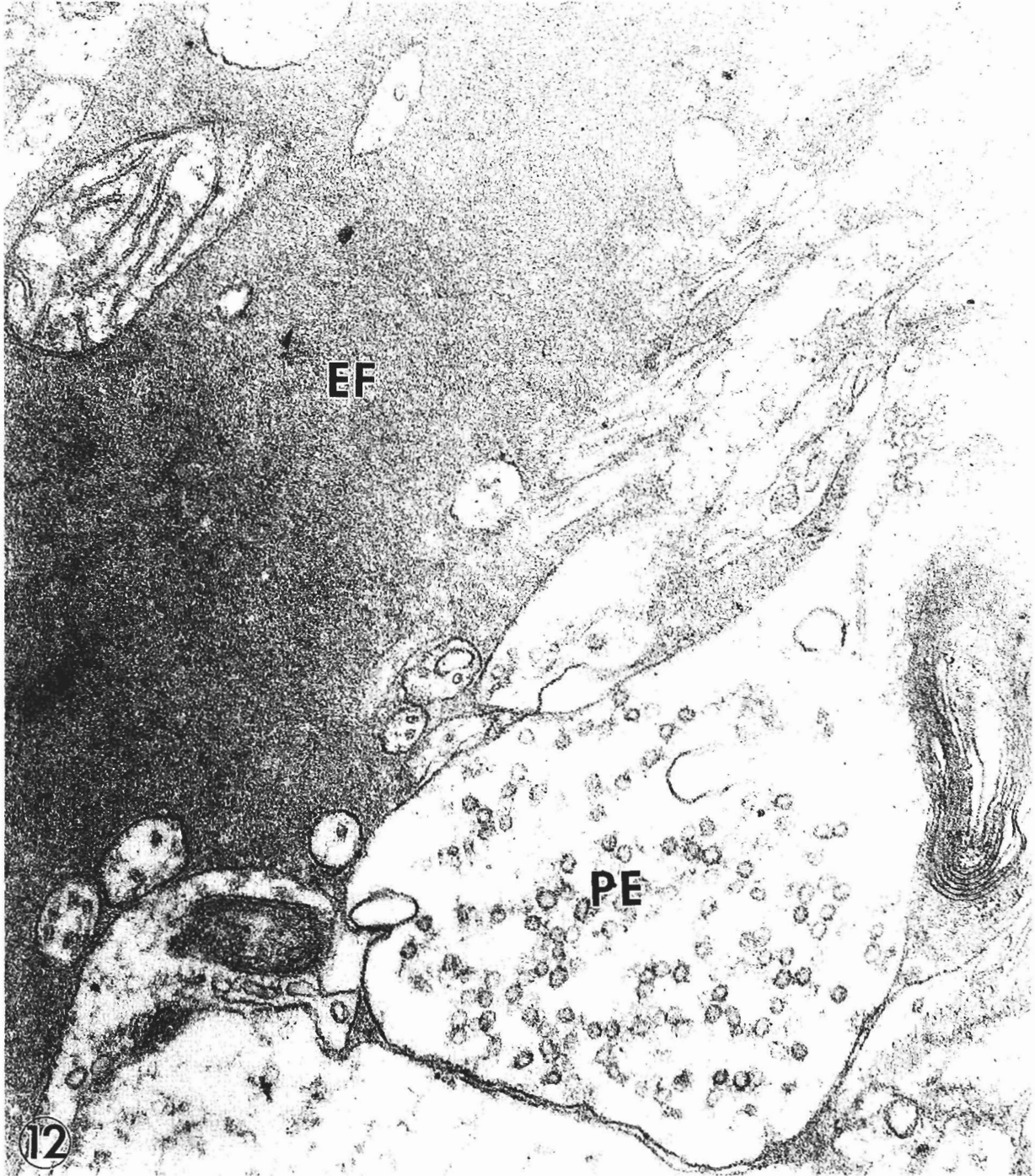


Fig. 12. Case No. 11. Left frontal haematoma. Left frontal cortex. Severe oedema. Ultrathin section showing dense proteinaceous hematogenous oedema fluid (EF) infiltrated in the extracellular space and dissociating a presynaptic ending (PE), containing spheroidal synaptic vesicles, from undifferentiated nerve cell processes in the neuropil. x 60,000

Extensive areas containing dense proteinaceous oedema fluid, with or without fibrin organization, were also found in other severely oedematous regions (Fig. 12).

Swollen dense oligodendrocytes were also identified associated to degenerated myelinated axons (Fig. 13) in semithin sections of oedematous parietal cortex examined by (S)TEM. Phagocytic astrocytes and dark ischaemic oligodendrocytes were also found in semithin sections examined by the (S)TEM mode (Fig. 14).

In ultrathin sections of the anoxic-ischaemic regions of the parietal cortex examined by TEM, glycogen-rich

astrocytes were observed, containing numerous, type glycogen granules (Fig. 15). In these regions, glycogen-depleted astrocytes were also present (Fig. 16), exhibiting a clear, translucent cytoplasm, fragmented Golgi complex and containing few, isolated, type β glycogen granules (Fig. 17).

In severe oedema, hydropic perivascular and interfascicular oligodendrocytes showing a dense nucleus, vacuolar enlargement of endoplasmic reticulum and perinuclear cistern and swollen mitochondria, were frequently observed (Fig. 18).

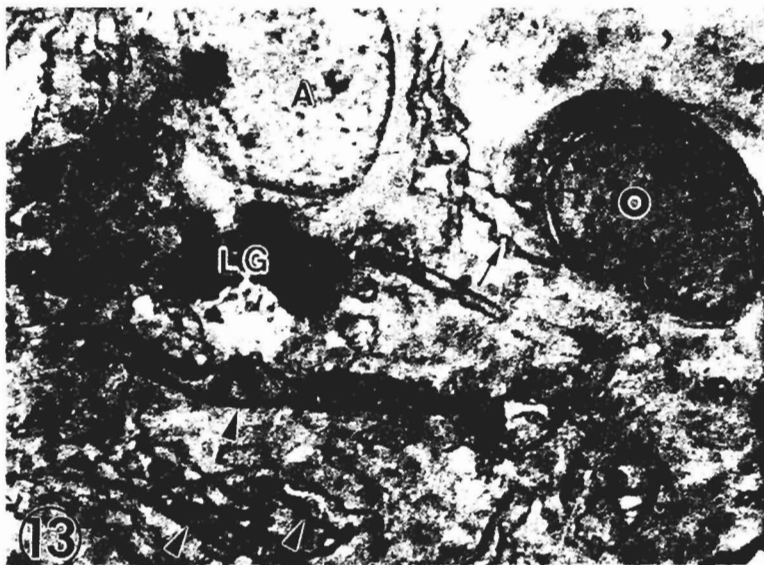


Fig. 13. Case No. 10. Left parieto-occipital subdural hygroma. Scanning-transmission electron micrograph of an Epon unstained semithin section of moderately oedematous parieto-temporal cortex. A clear swollen astrocyte (A) and a dense swollen oligodendrocyte (O) are seen. The astrocyte exhibits lipofuscin granules (LG) and the oligodendrocyte appears associated to a degenerated myelinated axon (arrow). Numerous degenerated myelinated axons (arrowheads) are also seen in the neighboring neuropil. x 2,500

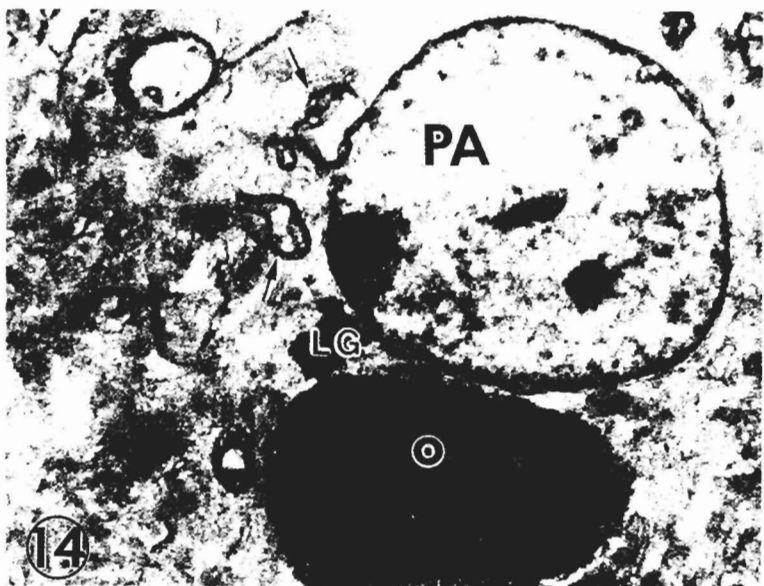


Fig. 14. Case No. 10. Left parieto-occipital subdural hygroma. Scanning-transmission electron micrograph of an Epon unstained semithin section of left parieto-temporal cortex with moderate oedema. A phagocytic astrocyte (PA) with engulfed myelinated axons (arrows) and a lipofuscin granule (LG) is observed. A dark oligodendrocyte (O) with a pyknotic nucleus is also seen. x 2,500

Discussion

In the present study we have carried out an intermicroscopic investigation, examining consecutively thick, semithin and ultrathin plastic sections of traumatic oedematous human cerebral cortical biopsies. The proposed goal was to identify with better resolution the vascular and nerve cell alterations involved in the genesis of vasogenic brain oedema.

As illustrated in Figs. 1 to 3, the impact energy of traumatic agents produced lesions of the capillary wall and primary formation of vasogenic brain oedema. The hematogenous oedema fluid escaped from the injured capillary wall, invaded the extracellular space of the brain parenchyma separating the nerve and neuroglial cell processes in the neuropil and also increasing the intracranial pressure. This fact in turn, resulted in impaired cerebral circulation and anoxic-ischaemic conditions of brain parenchyma inducing secondarily cytotoxic oedema (Kuroiwa et al., 1994; Castejón et al., 1997). A detailed description on the pathogenesis of traumatic human brain oedema has been published by means of microscopic techniques (Cervos-Navarro and Lafuente, 1991) and magnetic resonance

imaging (Marmorou et al., 2000). The net effect was the swelling of neuronal and neuroglial cells and subsequent degenerative and reactive processes. Astrocytic cells were the most damaged cells in both moderate and severe oedema. These later findings have been widely reported not only in experimental brain trauma (Bakay et al., 1977; Kimelberg and Norenberg, 1992; Kimelberg, 1995) but also in human brain trauma (Long et al., 1966; Manz, 1974; Castejón, 1980, 1998a,b).

The thick and semithin sections showed the perivascular haemorrhages and/or perivascular proteinaceous oedema fluid, and the ultrathin sections displayed open endothelial junctions, indicating the blood-brain barrier breakdown and the initial vasogenic nature of traumatic brain oedema (Castejón, 1985). In addition, the endothelial peripheral cytoplasm showed increased transcytosis process (Vasile et al., 1983; Sasaki et al., 1986; Milici et al., 1987; Michel and Curry, 1999), featured by augmented formation of vacuoles and micropinocytotic vesicles (Castejón, 1984a,b).

The light microscope study showed ischaemic dense pyramidal and non-pyramidal neurons and dense perineuronal and interfascicular oligodendrocytes. The semithin section and (S)TEM observation, and the

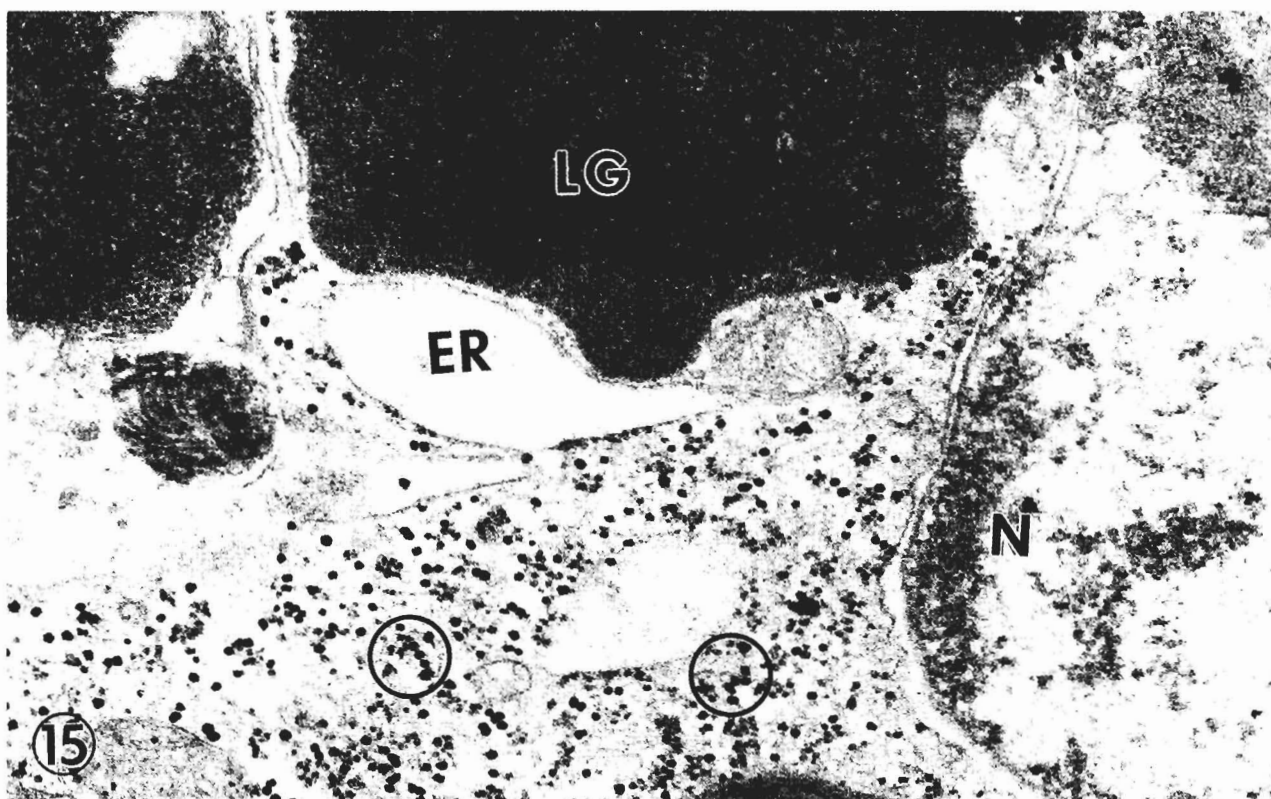


Fig. 15. Case No. 10. Left parieto-occipital subdural hygroma. Left parietal cortex. Moderate oedema. Ultrathin section of a glycogen-rich astrocyte showing, type glycogen granules (circles) and large lipofuscin granules (LG). The nucleus (N) is seen at the right side of the figure. x 60,000

ultrathin section and TEM study revealed the intraneuronal and intragial oedema of the cytoplasmic membrane compartment.

All microscopic methodologies employed revealed enlarged extracellular spaces responsible for the so called status spongiosus of brain parenchyma. Notably, oedematous astrocytes and phagocytic astrocytes were also observed. An interesting finding was the presence of glycogen-rich and glycogen-depleted astrocytes in anoxic-ischaemic regions which suggests anaerobic mobilization of glycogen stores (Castejón, 1999), rapidly depleted during anoxia (Philbin and Ransom, 1993) and an active participation of astrocytes in energy metabolism of ischaemic neurons and oligodendroglial cells.

The degenerative process of oligodendrocytes is a controversial issue reported by some investigators (Bresnahan et al., 1996; Castejón, 1998b), and denied by others (Kimelberg, 1995). In the present study (S)TEM examination of brain parenchyma positively confirmed the oligodendrocyte changes in human brain trauma. This subject has been recently reported in detail elsewhere (Castejón and Castejón, 2000).

Scanning transmission electron microscopy of plastic semithin sections of brain parenchyma offers the following advantages: 1) Quick specimen preparation for observation at low magnification. 2) Rapid analysis of large areas of brain parenchyma in which all cellular structures can be simultaneously visualized. 3) Better specimen preservation than material embedded in

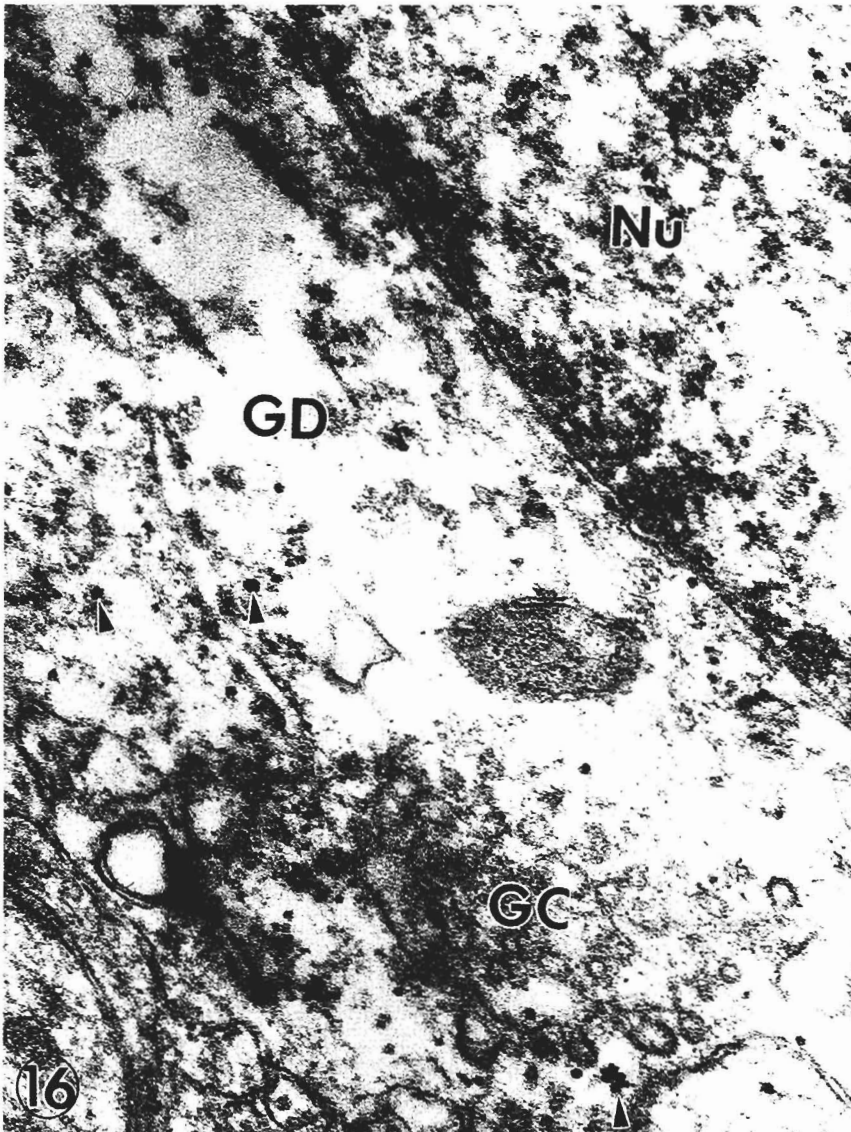


Fig. 16. Case No. 10. Left parieto-occipital subdural hygroma. Left parietal cortex. Moderate oedema. Ultrathin section of a glycogen-depleted astrocyte (GD) showing a clear, electron translucent cytoplasm and a vesicular type Golgi complex (GC). Few isolated, type glycogen granules still persist (arrowheads). The nucleus (Nu) is observed in the right upper corner of the figure. x 60,000

paraffin for light microscopy. 4) Previous adequate tissue information before ultrathin sectioning for TEM, conventional (CSEM) and high resolution scanning electron microscopy (HRSEM). 5) Better resolution and higher magnification for characterizing subtle pathological alterations.

In the present report we have examined and compared the alterations of neurons and neuroglial cells by light microscopy of toluidine blue-stained plastic thick sections and by (S)TEM of similar, unstained and uncoated semithin plastic sections. The proposed goal was to identify with better resolution the alterations of nerve cells and to trace the intraparenchymatous course of oedema fluid with a quick, reliable method and at a magnification higher than that obtained with the routine light microscopy study of paraffin-embedded material. As mentioned above, such study in thick plastic sections is also important as an intermediate step to conventional and high resolution SEM investigations. Besides, this method allows us to correlate light microscopy and scanning-transmission electron images. An entire area of the cortical biopsy can be observed by both methods. In general, the (S)TEM image is generated as the conventional secondary electron image (Zeitler, 1971).

The image contrast obtained in the (S)TEM mode is more accurate for identifying cellular alterations than that observed with LM in toluidine blue-stained thick sections.

As shown in the present study, the (S)TEM and TEM methodologies offer the adequate resolution to clearly distinguish moderate from severe oedema in the analysis of traumatic injuries of brain neuropil. A slightly dilated extracellular space separating nerve cell processes was found in moderate oedema, and large, distended vacuolar spaces featured the severe oedema. In a previous study we have shown by means of LM and TEM the ultrastructural pathology of moderate and severe brain oedema (Castejón et al., 1997). The finding of shrunken and high electron dense pyramidal and non-pyramidal neurons establishes the degree of degeneration induced by the traumatic agent and also by the associated vasogenic and cytotoxic brain oedema. The increased electron density of ischaemic and degenerated oligodendroglial cells and the degeneration of myelinated axons express the associated and intimated relationship between these structures and the dysfunction of the nursing role exerted by oligodendroglial cells upon myelinated axons.

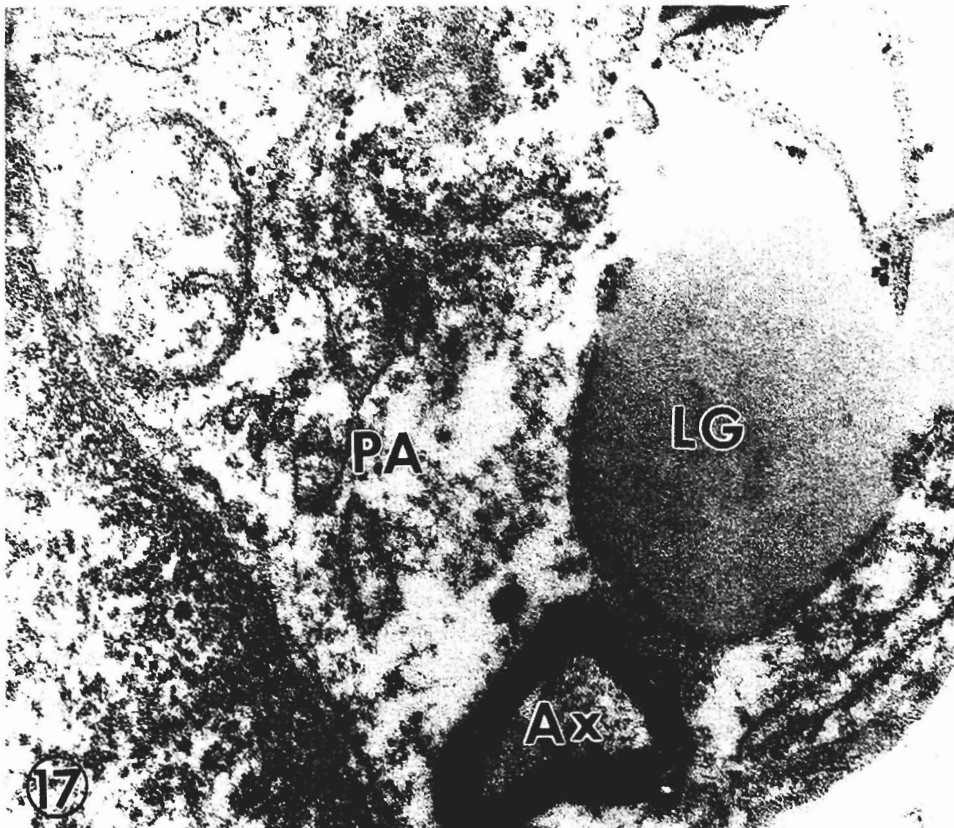


Fig. 17. Case No. 11. Left frontal haematoma. Left frontal cortex. Severe oedema. Ultrathin section of a phagocytic astrocyte (PA) showing an engulfed myelinated axon (Ax) and a lipofuscin granule (LG). x 60,000



Fig. 18. Case No. 11. Left frontal haematoma. Left frontal cortex. Severe oedema. Ultrathin section of a dense hydropic oligodendrocyte showing a dense nucleus (Nu), a remarkable enlargement of endoplasmic reticulum (ER) and perinuclear cistern (arrowheads) and swollen mitochondria (M). x 60,000

Acknowledgements. This work has been carried out by a subvention obtained from CONDES-LUZ. Thanks are due to Laura Villamizar for invaluable secretarial help and to Ralph Caspersen for skilled technical assistance.

References

- Bakay I., Lee J.C. and Peng J.R. (1977). Experimental cerebral concussion. Part I: An electron microscopic study. *J. Neurosurg.* 47, 525-553.
- Boyde A. and Reid S.A. (1983). A new method of scanning electron microscopy for imaging biological tissues. *Nature* 302, 522-523.
- Bresnahan J.C., Shurman S.L. and Beattie M.S. (1996). Evidence for apoptosis of oligodendroglia in long tracts undergoing degeneration after spinal cord injury (SCI) in monkey. *Soc. Neurosci. Abst.* Vol. 2. Part 2, p. 1185.
- Brockmeyer C., Thiedemann K.U. and Morh U. (1989). An improved embedding method for obtaining semithin and ultrathin sections from critical-point dried trachea specimens. *Exp. Pathol.* 36, 233-236.
- Cajander S.B. (1986). A rapid and simple technique for correlating light microscopy, transmission and scanning electron microscopy of fixed tissues in Epon blocks. *J. Microsc.* 143, 265-274.
- Castejón O.J. (1980). Electron microscopic study of capillary wall in human cerebral edema. *J. Neuropathol. Exp. Neurol.* 49, 296-328.
- Castejón O.J. (1984a). Increased vesicular and vacuolar transport in traumatic human brain edema. A combined electron microscopic study and theoretical approach. *J. Submicrosc. Cytol.* 16, 359-369.
- Castejón O.J. (1984b). Formation of transendothelial channels in traumatic human brain edema. *Pathol. Res. Pract.* 179, 7-12.
- Castejón O.J. (1985). Electron microscopic observations of endothelial junctions in perifocal human brain edema. An interpretative study. *J. Submicrosc. Cytol.* 17, 105-114.
- Castejón O.J. (1998a). Morphological astrocytic changes in complicated human brain trauma. A light and electron microscopic study. *Brain Injury* 12, 409-427.
- Castejón O.J. (1998b). Electron microscopic analysis of cortical biopsies in patients with traumatic brain injuries and dysfunction of neurobehavioural system. *J. Submicrosc. Cytol. Pathol.* 30, 145-156.
- Castejón O.J. (1999). Astrocyte subtype in the gray matter of injured human cerebral cortex: a transmission electron microscope study. *Brain Injury* 13, 291-304.
- Castejón O.J. and Castejón H.V. (2000). Oligodendroglial cell behaviour in traumatic oedematous human cerebral cortex: a light and electron microscopic study. *Brain Injury* 14, 303-317.
- Castejón O.J., Valero C. and Díaz M. (1997). Light and electron microscope study of nerve cells in traumatic oedematous human cerebral cortex. *Brain Injury* 11, 363-388.
- Cervos-Navarro J. and Lafuente J.V. (1991). Traumatic brain injuries: structural changes. *J. Neurol. Sci. (Suppl)* 103, 3-14.
- De Nee P.B., Frederickson R.G. and Pope R.S. (1977). Heavy metal staining of paraffin, epoxy and glycol methacrylate embedded biological tissue for scanning microscopy histology. *Scanning Electron Microscopy I*, 83-92.
- Ito E., Kudo R., Miyoshi M., Tanaka S., Kumai K., Takashina T. and Hashimoto M. (1988). Transmission and scanning electron microscopic study of the same cytologic material. *Acta Cytol.* 32, 588-592.
- Keyse R.J., Garrat-Reed A.J., Goodhew P.J. and Lorimer G.W. (1998). Introduction to scanning transmission electron microscopy. Bios Scientific Pub. Springer-Verlag. New York. pp 1-10.
- Kimelberg H.K. (1995). Brain edema. In: Neuroglia. Kettenmann H. and Ramson B.R. (eds.). Oxford University Press. New York. pp 919-935.
- Kimelberg H.K. and Norenberg M.D. (1994). Astrocyte response to CNS trauma. In: Neurobiology of central nervous system trauma. Salzman S. and Faden A. (eds.). Oxford University Press. New York. pp 193-208.
- Kuroiwa T., Ueki M., Chen A., Suemasu H., Taniguchi I. and Okeda R. (1994). Biomechanical characteristics of brain edema: the difference between vasogenic-type and cytotoxic-type edema. *Acta Neurochir. Suppl. (Wien)* 60, 158-161.
- Kushida T., Nagato T. and Kushida H. (1977). Observation on the same place in semi-thin section with both light and electron microscopy. *J. Electron Microscop.* 26, 345-348.
- Long D.M., Hartman I.F. and Freveh L.A. (1966). The ultrastructure of human cerebral edema. *J. Neuropathol. Exp. Neurol.* 25, 373-395.
- Manz H.J. (1974). The pathology of cerebral edema. *Human Pathol.* 5, 291-313.
- Marmorou A., Fatouros P.P., Barzo P., Portella G., Yoshihara M., Tsuji Yamamoto T., Laine F., Signoretto S., Ward J.D., Bullock M.R. and Young H. (2000). Contribution of edema and cerebral blood volume to traumatic brain swelling in head-injured patients. *J. Neurosurg.* 93, 183-193.
- Michel C.C. and Curry F.E. (1999). Microvascular permeability. *Physiol. Rev.* 79, 703-761.
- Mikel U.V. and Johnson F.B. (1980). A simple method for study of the same cells by light and scanning electron microscopy. *Acta Cytol.* 24, 252-254.
- Milici A.J., Watrous N.E., Stukenbrok H. and Palade G.E. (1987). Transcytosis of albumin in capillary endothelium. *J. Cell Biol.* 105, 2603-2612.
- Nagato Y., Kushida T., Kushida H. and Ogura K. (1983). Observation on backscattered electron image (BEI) of a scanning electron microscope (SEM) in semi-thin sections prepared for light microscopy. *Tokai J. Exp. Clin. Med.* 8, 167-174.
- Ogura K. and Laudate A. (1980). Comparative observations with a light microscope and a SEM backscattered electron model. *Scanning Electron Microscop.* III, 233-238.
- Oka Y., Satou M. and Ueda K. (1987). An improved method for correlative light and electron microscopic examination of cobaltic-labeled neurons. *Neurosci. Lett.* 73, 187-191.
- Pasquinelli G., Scala C., Borsetti G.P., Martegani F. and Laschi R. (1985). A new approach for studying semithin sections of human pathological material: intermicroscopic correlation between light microscopy and scanning electron microscopy. *Scanning Electron Microscop.* III, 1133-1142.
- Pavlik L.L., Moshkov D.A. and Udaltsov S. N. (1986). Detection of giant axospinal synapses in the hippocampus on semithin sections. *Tsitologiya* 28, 1005-1007.
- Philbin D.M. and Ransom B.R. (1993). Anoxia induced extracellular ion shifts in mammalian CNS white matter. In: Biology and pathology of astrocytes-neuron interaction. Federoff S., Benhard H.J., Juurlink H.J. and Ronred D. (eds). Plenum Press. New York. pp 27-50.
- Phillips D.M. (1998). Electron microscopy: use of transmission and scanning electron microscopy to study cells in culture. *Methods Cell*